Pressure measurement in two-dimensional horizontal granular gases

J.-C. Géminard and C. Laroche
Laboratoire de Physique de l'E.N.S. de Lyon, 46 Allée d'Italie, 69364 Lyon Cedex 07, France
(Received 7 January 2003; revised manuscript received 20 May 2004; published 11 August 2004)

A two-dimensional granular gas is produced by vibrating vertically a partial layer of beads on a horizontal plate. Measurements of the force applied by the granular gas to the sidewalls of the container, or granular pressure, are used to study the effect of the shaking strength, density, bead-plate restitution coefficient, and particle size on the steady properties of the gas.

DOI: 10.1103/PhysRevE.70.021301 PACS number(s): 45.70.−n, 45.50.Tn, 51.10.+y, 64.90.+b

I. INTRODUCTION

The collective behavior of dry solid grains is of practical importance for various applications in industry; transport, storage, or mixing are often involved in handling of industrial powders and problems arise when the grains form a blockage in a pipe, blow up a container or segregate. Granular materials exhibit a rich and intriguing phenomenology which has been the subject of intensive research for the last two decades [1–3]. The static and dynamic unusual behavior of these systems is mainly due to the nonlinear, hysteretic, and dissipative nature of the contacts between the solid grains; within a sandpile at rest, the forces are transmitted through a heterogeneous network of contacts that brings into play the nonlinearity of the Hertz contact [4] as well as the solid friction between the grains [5]. Within all kinds of granular flows, inelastic collisions between particles occur, leading to intrinsic dissipation. There have been numerous experimental, numerical and theoretical studies of the dynamics of large collections of inelastic particles in motion [1–3,6–11].

In order to explore experimentally the effects of the dissipation on the properties of granular systems, it is convenient to produce stationary states; they are achieved by continuously providing the system with energy, compensating the energy lost when the grains are in motion. The energy source can consist of a continuous fluid flow leading to the fluidization of the granular material [12], of an ac electric field imposed to charged grains [13,14], of a periodic forcing of one of the sidewalls [15,16], or of a vertical or horizontal vibration of the whole container (see [1–3] for review). We are interested here in the case of two-dimensional (2D) granular gases consisting of a horizontal partial layer of inelastic beads driven by a vertically vibrating boundary. We consider the case of large enough beads for the air-drag force to be negligible; the energy dissipation within the gas only results from the inelastic bead-bead collisions. This experimental situation has been realized by Olafsen and Urbach [17,18], and by Losert, Gollub and co-workers [19,20]. In addition, it has been the framework of molecular-dynamics simulations by Nie, Ben-Naim, and Chen [21]. The experimental studies focused on the density fluctuations and velocity distributions [18,19], on clustering and collapse [17], and on front propagation [20]. However, whereas particle tracking was successfully used to measure correlations between local quantities, only a few results make it possible to discuss the effects of the bead-plate restitution coefficient, ϵ, and bead diameter, D, on global quantities like the granular temperature or granular pressure.

We make use of an alternative experimental method for analyzing the influence of the plate acceleration, Γ, number density, ρ, restitution coefficient, ϵ, and bead diameter, D, on the steady properties of the granular gas; we measure the force applied, per unit length, by the granular gas to the sidewalls of the container, or granular pressure, P.

II. EXPERIMENTAL SETUP

The experimental setup (Fig. 1) consists of a horizontal tray (surface area $S=10\times 10$ cm^2, thickness 6 mm) undergoing harmonic oscillations in the vertical direction according to $z(t)=A\cos(2\pi\nu t)$ with, A, the vibration amplitude, and, $\nu=\omega/2\pi$, the frequency. The vertical motion is imposed with the help of an electromagnetic shaker (Brüel and Kjaer, type 4803) driven by sine waves ($\nu=50-80$ Hz) from a low distortion signal generator (Stanford Research Systems, DS345) and a power amplifier (Kepco, BOP50-4M). The vibration strength can be characterized by the peak velocity $v_p=A\omega$, or by the dimensionless acceleration $\Gamma\equiv A\omega^2/g$, where g is the acceleration due to gravity. The amplitude A of the vertical oscillation is measured by an inductive sensor (Electrocorp,

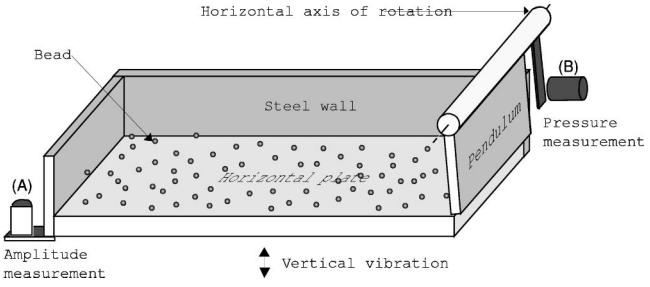

FIG. 1. Experimental setup. The experimental setup consists of a horizontal tray that oscillates sinusoidally along the vertical. The vertical displacement of the tray is measured with the help of an inductive sensor (A). Three of the sidewalls are attached to the horizontal plate, whereas the last one (the pendulum, on the right-hand side) rotates freely around a horizontal axis, which is fixed in the laboratory frame. The angle that the pendulum makes with the vertical direction is measured with the help of a second inductive sensor (B).

TABLE I. Bead-plate restitution coefficient ϵ.

	Dural	Steel	Brass	Copper
Glass beads	0.83	0.95	0.92	0.76
Steel beads	0.88	0.91	0.84	0.79

EMD1053), so that Γ (ranging from 0 to 3) is known within 0.01.

The granular gas consists of a large number ($N=200-3500$) of beads (diameter $D=1.5$, 2, 2.5, 3, and 3.5 mm) placed in the tray. The beads are made of steel (Marteau and Lemarié, AISI) or glass (Marteau and Lemarié, glass). We define the coverage

$$C \equiv N/N_{\max} = \frac{\sqrt{3}}{2}\frac{D^2}{S}N, \tag{1}$$

where $N_{\max}$ denotes the maximum number of beads in a monolayer which covers the whole surface of the horizontal plate. We limit our study to coverages $\mathcal{C}$ ranging from 0.2 to 0.5. With m the mass of one bead, we denote $M=Nm$ the mass of N beads, and $\rho \equiv N/S$ the corresponding number density.

The restitution coefficient ϵ characterizing the collisions between the beads and the plate (Table I) is measured by recording the successive collision times t_n of a single bead bouncing vertically on the plate at rest [22]. The measurements are performed for bouncing heights similar to those observed in the experiments (typically 1 mm). The times t_n are detected by recording the signal from one accelerometer attached to the horizontal plate with a digitizing oscilloscope (Nicolet, 4094C). Assuming that ϵ does not depend on the bouncing velocity, one expects the relation

$$\ln(t_{n+1} - t_n) = K + n \ln(\epsilon), \tag{2}$$

where K is a constant. The linear interpolation of $\ln(t_{n+1} - t_n)$ as a function of n gives ϵ to within 0.03 (Table I). We point out that ϵ does not exhibit any dependence on the diameter D of the beads, as expected for a bead bouncing over a thick plate. However, in practice, ϵ is not constant; it increases continuously when the impact velocity decreases, and approaches unity when the impact velocity vanishes [22,23]. Moreover, we do not take into account the rolling or sliding frictions plausibly involved in the bead-bead or bead-plate contacts [24,25]. The values of the restitution coefficients e characterizing the bead-bead collisions have not been measured but one can estimate $e \simeq 0.95$ [26].

The pressure measurements are performed by means of a pendulum (Fig. 1). Three of the vertical sidewalls (steel plates, height 3 cm, thickness 2 mm) are attached to the horizontal plate. The top edge of the fourth wall (the pendulum) is attached to a rod that rotates without any significant solid friction around its horizontal axis which remains motionless in the laboratory frame. In order to avoid the beads escaping the system, the vertical distance between the bottom edge of the pendulum and the top surface of the horizontal plate has been chosen to be of about 0.2 mm, smaller than the radius $D/2$ of the smaller beads used in our experiments. We measure the horizontal distance between the bottom edge of the pendulum and a second inductive sensor (Electrocorp, EMD1053, Fig. 1), so that the instantaneous tilt angle, $\theta(t)$, that the pendulum makes with the vertical axis is known to be within 10^{-4} rad. When beads are vibrated in the tray, because of beads colliding with the pendulum, the angle $\theta(t)$ (always less than 2°) fluctuates (typical frequency 1 Hz, much less than the vibration frequency ν) around a nonzero mean value $\langle\theta\rangle$. The small fluctuations of $\theta(t)$ could influence back the properties of the gas; we checked that further damping the oscillations does not change the average angle of deflection $\langle\theta\rangle$. (A vertical rod is attached to the pendulum and immersed at its bottom edge in a viscous oil.) Let F be the force applied per unit length by the gas to the pendulum. Assuming that F is applied at the bottom edge of the pendulum and neglecting any inertial effect, one can show that the relation between F and $\langle\theta\rangle$ is

$$F = \frac{\mathcal{M}g}{2}\langle \sin\theta(t)\rangle \simeq \frac{\mathcal{M}g}{2}\langle\theta\rangle \quad (\theta \ll 1 \ \ \forall \ \ t), \tag{3}$$

where $\mathcal{M}$ is the mass of the wall per unit length and g the acceleration due to gravity. Let H_b be the typical bouncing height of the beads above the horizontal plate and H be the total height of the pendulum ($H=3$ cm). For a given measured mean angle $\langle\theta\rangle$, the gas applies to the pendulum the mean horizontal force, or granular pressure, $P \simeq FH/(H-H_b)$. As H_b never exceeds $H/10$, the discrepancy between F and P is always less than 10% and we will assume $P=F$ in the following (the amplitude A which never exceeds 0.3 mm$=H/100$ can always be neglected). Thus, averaging $\theta(t)$ during 5 min at 1 Hz makes it possible to determine $\langle\theta\rangle$ to within 10^{-4} rad. In our experimental conditions, $P=(2.4\langle\theta\rangle)\pm 3\times 10^{-4}$ N/m.

The horizontality of the surface is insured by checking that the collapse, a condensate of motionless particles that appears at low shaking strength, nucleates randomly on the plate surface. In addition, we check that the acceleration is vertical and homogeneous over the whole surface by the use of accelerometers (PCB-303A) placed at different locations along the sides of the plate; in order to insure that the inertia of the beads does not affect the adjustment of the experimental setup, these verifications are performed with the beads in the tray. Neither the acceleration difference between two corners of the setup nor the horizontal acceleration exceed 0.01 g.

III. EXPERIMENTAL RESULTS

A. Experimental procedure

The experimental procedure is as follows: A large number N of beads is placed in the tray and the vibration amplitude A is set to a large value (typically $A \simeq 0.18$ mm, corresponding to $\Gamma \simeq 2.5$ at $\nu=60$ Hz) so that the beads initially exhibit a homogenous gaseous state (Fig. 2). Afterwards, A is decreased step by step at constant frequency ν ($\nu=60$ Hz, except when specified). The pressure in the steady state P is

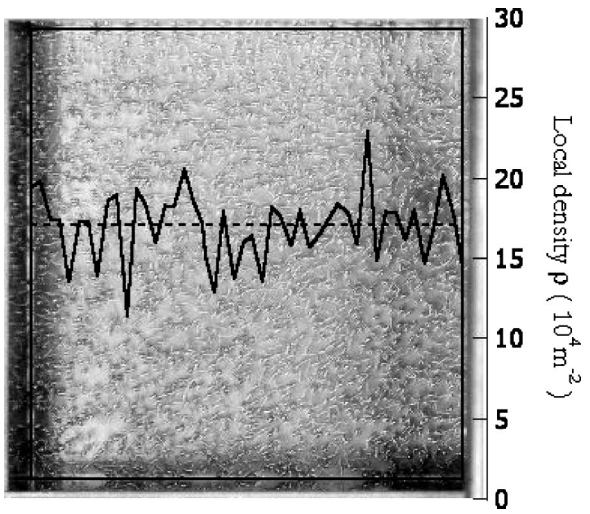

FIG. 2. Photograph of the gas and density profile. The density profile is obtained by counting the number of beads in rectangular regions of the tray (2 mm×10 cm, the long edge parallel to the pendulum). At large acceleration, the granular gas is homogeneous; the density profile (black curve) does not show any increase of the density close to the sidewalls, including the pendulum (on the right-hand side). The black box marks the limits of the horizontal plate (images of beads that appear to be outside the box are due to reflections from the steel walls). The image comes from a standard charge coupled device (CCD) camera placed above the experimental setup (exposure time 1/1000 s, sine wave, 60 Hz, $\Gamma=2$, steel beads, $D=1.5$ mm, Dural tray).

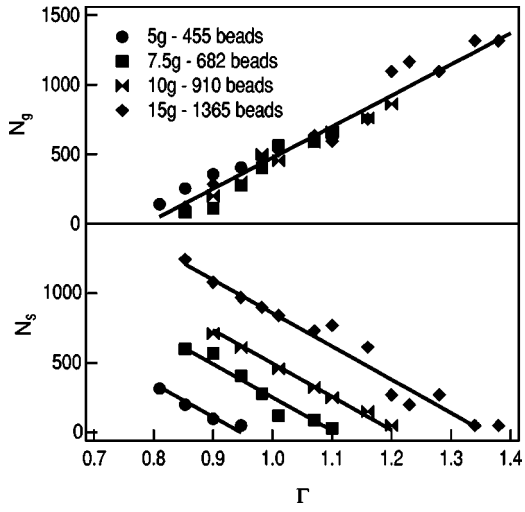

FIG. 3. Number of beads in the collapse N_s and in the gas N_g vs dimensionless acceleration Γ. Bottom: Number of beads in the collapse N_s vs Γ for different total number N of beads in the system; top: corresponding number of beads N_g in the gas. [We report the average over five experimental realizations. The accuracy is given by the scatter of the experimental data (sine wave, 60 Hz, glass beads, $D=2$ mm, Dural tray).]

measured at each acceleration Γ. A slight drift of the measurements can be observed when starting the experiment with a new plate; in order to avoid aging induced by the wear of the plate surface, we maintain the system in the gas phase ($\Gamma\sim 2$) for several hours (typically 12 h) before any set of experiments. After this preparation of the surface and after cleaning of the beads, no drift of the experimental results is observed. The restitution coefficient ϵ is measured after this preparation of the plate surface which does not seem to increase significantly the surface roughness; indeed, a bead that initially strikes the horizontal plate along the vertical does not experience any significant horizontal motion.

B. First visual observation: Clustering and collapse

Direct observation of the gas makes it possible to distinguish qualitatively, at least, four different regimes. At large acceleration (typically $\Gamma>1.2$, Fig. 2), the gas is homogeneous and all the beads seem to experience the same typical random motion (fully developed gas). At slightly lower accelerations, we observe the coexistence of slow beads and fast beads, described in Refs. [17,20] as the clustering phase. We again point out that clustering is not necessarily accompanied by the formation of a visible collapse. The collapse, described as a condensate of motionless particles that remain in contact with the plate and each other, generally nucleates when the acceleration is further decreased (the threshold will be discussed in the following). Finally, isolated beads can stop moving at lower accelerations (typically $\Gamma\simeq 0.6$). We will refer to this last situation as the frozen state.

We measured the number of beads within the collapse, N_s, as a function of Γ and ρ. Glass beads ($D=2$ mm) are vibrated on a Dural tray (surface area $S=10\times 10$ cm^2, $\epsilon\simeq 0.83$), and imaged from above with the help of a standard CCD video camera. As N_s fluctuates significantly even when the steady state is reached, we count the beads in the gas, N_g, and in the collapse, N_s, on still images. (We quench the system by setting A to zero and perform the measurements on live images from the camera. The surface area of the collapse does not change significantly during the sudden "cooling" of the system.) The experimental results are shown in Fig. 3. Below a threshold acceleration Γ_s, which depends on ρ, N_s increases linearly when Γ is decreased. Within the scatter of the experimental data, the slope does not depend on ρ. For a given Γ, the number density in the gas $\rho_g=N_g/S$ is given, and increases linearly with Γ according to $\rho_g=\eta(\Gamma-\Gamma_0)$ provided that the collapse exists [from the experimental data, $\Gamma_0=0.79\pm 0.1$ and $\eta=(2.23\pm 0.01)\ 10^5$ m^{-2}]. As a consequence, Γ_s increases linearly with ρ according to $\Gamma_s=\Gamma_0+\rho/\eta$.

When steel beads are used in place of glass beads, the acceleration Γ_s is shifted to lower values, and we observe that, for intermediate coverage ($C\sim 0.2-0.5$), the system is more likely to freeze (isolated beads stop moving) than to form a well developed collapse at low Γ. Moreover, even for the largest values of the coverage, the size of the collapse fluctuates significantly, making impossible reliable measurements. Nevertheless, steel beads exhibit qualitatively the same type of collapse-gas equilibrium.

C. Pressure measurements

1. Pressure P versus acceleration Γ

For a given vibration frequency ν, P decreases when A, and hence Γ, is decreased (Fig. 4). The pressure $P(\Gamma)$ exhib-

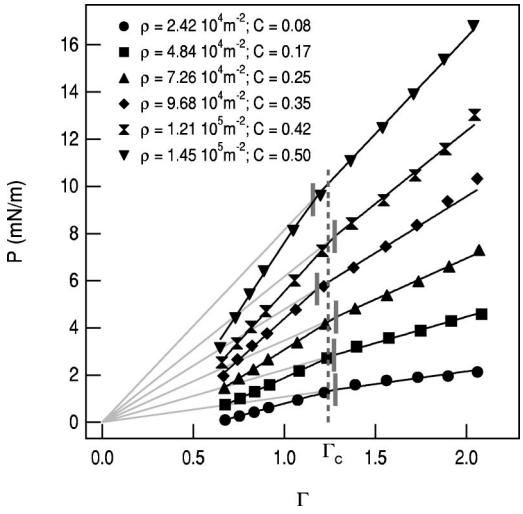

FIG. 4. Pressure P vs dimensionless acceleration Γ. Symbols correspond to the experimental data obtained for different number density ρ; black curves: interpolation of the data by two lines; gray solid lines: $P \propto \Gamma$ for $\Gamma > \Gamma_c$; gray vertical dashes: Γ_c for each density ρ; vertical dashed line: average value of Γ_c. For $\Gamma > \Gamma_c$, P is approximately proportional to Γ, whereas it goes approximately linearly to zero for $\Gamma < \Gamma_c$. The critical dimensionless acceleration Γ_c does not systematically depend on the density ρ (sine wave, 60 Hz, steel beads, $D=2$ mm, Dural tray).

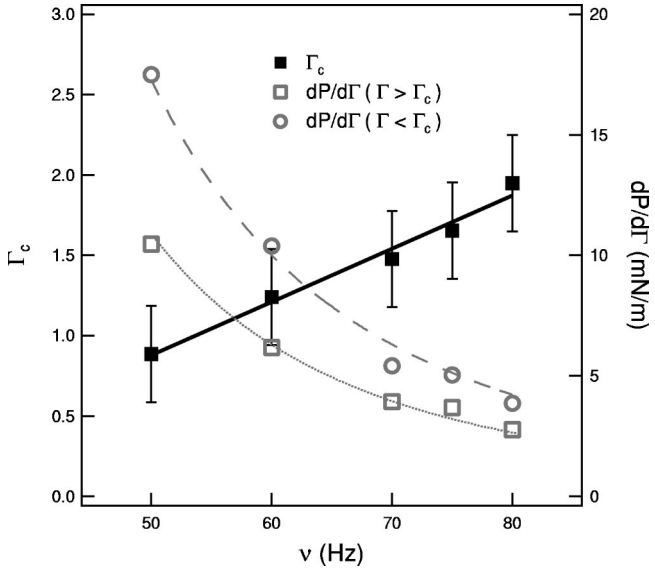

FIG. 5. Acceleration Γ_c and slope $dP/d\Gamma$ vs frequency ν. Full squares: critical acceleration Γ_c; plain line: best linear fit to $\Gamma_c \propto \nu$. Open squares: slope $dP/d\Gamma$ for $\Gamma > \Gamma_c$. Open circles: slope $dP/d\Gamma$ for $\Gamma < \Gamma_c$. The dotted and dashed lines correspond to the best fit to $dP/d\Gamma \propto \nu^{-3}$ (sine wave, steel beads, $\rho = 1.21 \times 10^5$ m^{-2}, $D=2$ mm, Dural tray).

its two different regimes. At large enough shaking strengths, P is approximately proportional to Γ. At intermediate shaking strengths, the slope increases and P is approximately linear in Γ. The transition is not marked by the appearance of a visible collapse. By contrast, the nucleation of a collapse at lower acceleration does not affect the curve $P(\Gamma)$. Further decreasing Γ, the limit $P \to 0$ cannot be reached experimentally. Indeed, when the acceleration is small (typically $\Gamma < 0.6$), the number of beads in motion becomes small. As a consequence, the number of beads colliding with the pendulum is drastically reduced, leading to a poor accuracy in the determination of the pressure. Moreover, the collapse can touch and stop the pendulum. Since the experimental setup fails to give reliable measurements of P when the frozen state is approached, we limit our measurements to $\Gamma > 0.65$.

Even if the transition between the two approximately linear regimes is not sharp, we can define a critical dimensionless acceleration, Γ_c, at which the transition occurs by interpolating the experimental data with two lines (Fig. 4); we assume that P is proportional to Γ for $\Gamma > \Gamma_c$, and that P increases linearly with Γ for $\Gamma < \Gamma_c$, together with the additional condition that the curve $P(\Gamma)$ is continuous. With this definition of the transition, Γ_c does not depend systematically on the density ρ, and $\Gamma_c = 1.24 \pm 0.07$ (sine wave, 60 Hz, steel beads, $D=2$ mm, Dural tray). From the experimental data, the pressure is expected to vanish at finite Γ (typically $\Gamma \simeq 0.3-0.4$).

In addition, we performed experiments for frequencies ν ranging from 50 to 80 Hz. The qualitative behavior of P as a function of Γ remains unchanged, whereas Γ_c and the slopes $dP/d\Gamma$ below and above Γ_c depend on the frequency (Fig. 5). The critical acceleration Γ_c is found to be proportional to ν, whereas the slopes $dP/d\Gamma$ scale approximately like ν^{-3}. As our study was limited to a narrow range of frequencies [27], these conclusions must be questioned. However, there is no doubt that Γ_c increases with ν, whereas P, at a given acceleration, drastically decreases when ν is increased.

The approximately linear dependence of P on A at a given ν is surprising at first sight. Indeed, the mean energy $\langle E_z \rangle$, associated with the vertical motion of an isolated bead bouncing on a horizontal vibrating plate, is often assumed to scale like v_p^2. In this case, at a given frequency, $\langle E_z \rangle$ would scale like A^2. We have suggested that $\langle E_z \rangle$ depends linearly on A at small accelerations [29]. Thus, if the mean square horizontal velocity $\langle v^2 \rangle$ of the particles within the 2D gas is proportional to $\langle E_z \rangle$ associated to their vertical motion, the linear dependence of P on A is likely to be simply due to the dependence of $\langle E_z \rangle$ on the shaking strength. The scaling $P \propto v_p^2$ would then be observed only at larger accelerations (typically $\Gamma > 3$).

2. Pressure P versus number density ρ

One can expect P to be roughly proportional to ρ. Indeed, considering the momentum balance for the beads striking the wall, one can write

$$P \simeq \frac{1+\epsilon'}{4} \rho m \langle v^2 \rangle, \tag{4}$$

where ϵ' is the velocity restitution coefficient characterizing the bead-wall collisions and v the horizontal velocity of the beads. The relation (4) is relevant only at large enough accelerations, when the system remains homogeneous (i.e., not subjected to any clustering, collapse or accumulation of

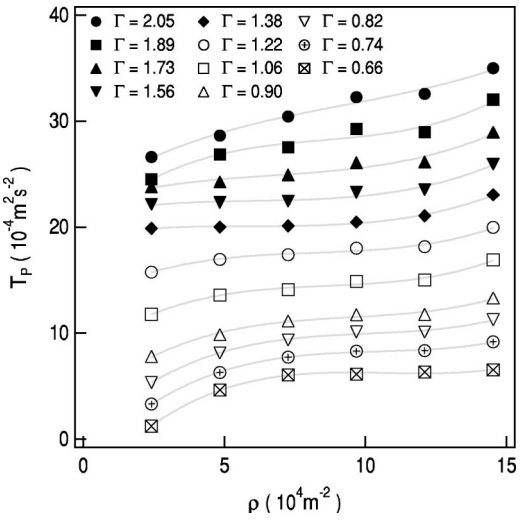

FIG. 6. T_P vs number density ρ. The value of T_P is deduced from Eq. (4) and from the experimental data of the Fig. 4. The lines are guides to the eye. The open symbols point out the condition $\Gamma<\Gamma_c$ whereas the full symbols correspond to $\Gamma>\Gamma_c$. (sine wave, 60 Hz, steel beads, $D=2$ mm, Dural tray).

beads close to the wall). We measured for steel beads colliding with a steel plate, $\epsilon'=0.91$ (Table I). This value of ϵ' is large enough for the beads not to accumulate significantly close to the wall (Fig. 2). From the data of Fig. 6, we calculate the quantity $T_P \equiv P/(m\rho)$ and find that T_P increases slightly with increasing ρ for all acceleration, whether or not the system is homogeneous. Provided that the relation (4) holds true, these results are compatible with a slight increase of the mean kinetic energy per particle, associated with the horizontal motion, with ρ.

For a given bead diameter D, Γ_c seems to correspond to a well defined value of T_P, independent of the density ρ. We found in Sec. III C 1 that $\Gamma_c \propto \nu$, whereas $dP/d\Gamma \propto \nu^{-3}$. Even if these scaling laws can be questioned, we can deduce that $T_P \propto \nu^{-2}$ at Γ_c. We can guess that $H_b \propto T_P$; with this assumption, the dependence of Γ_c on ν is not compatible with a transition induced by a change in the dimensionality of the system. Indeed, $T_P(\Gamma_c)$ should correspond to $H_b \simeq D$ and then should not depend on ν. By contrast, with the same assumption, the typical frequency of the bead-plate collisions $\nu^* \propto 1/\sqrt{T_P}$. Thus the transition could correspond to a given ratio ν^*/ν and, hence, could be due to the existence of attractors to periodic motion at low accelerations [28,29].

In conclusion, at first sight, P is approximately proportional to ρ. However, T_P increases slightly when ρ is increased up to coverage $C \simeq 0.5$. This observation seems to indicate that, at small coverages $C<0.5$, the improvement of the energy transfer from the vertical to the horizontal motion dominates the increase of the energy loss due to the bead-bead collisions when ρ is increased. This conclusion agrees qualitatively with measurements of the granular temperature, T_G, performed by Losert *et al.* for small coverages [19]. Indeed, the authors report a slight increase in T_G with the density ρ at small coverage. However, we do not observe any decrease in T_P up to $C=0.5$ ($\rho=1.45\times10^5$ m^{-2}).

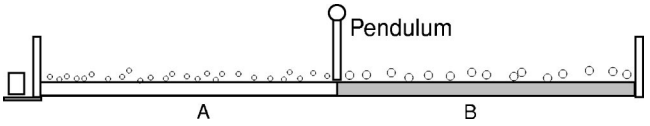

FIG. 7. Direct measurement of pressure difference. The pendulum separates the system in two compartments A and B having the same surface area. When beads are vibrated on both sides of the pendulum, one measures the pressure difference $P_A - P_B$ for exactly the same characteristics of the vertical vibration.

3. Pressure P versus bead diameter D

In order to compare accurately the changes in P induced by a change in D, we performed direct measurements of the pressure difference between two granular gases made of beads having different diameters D.

The experimental setup consists of a single vibrating plate (Dural, 20×10 cm^2), similar to that used in the previous sections, separated in two compartments A and B (surface area $\mathcal{A}=10\times10$ cm^2) by the pendulum (Fig. 7). The system hence makes possible the measurement of the pressure difference $\Delta P=P_A-P_B$ between two isolated granular gases at exactly the same Γ. The pressure P_A (P_B) is initially measured by keeping the beads in compartment B (A) from striking the pendulum; this is realized by placing an additional light wall close to the pendulum in compartment B (A). When the wall is removed, we measure ΔP. The experiment is repeated after swapping of the beads in compartments A and B.

The experimental results show that, at large Γ, P_A and P_B are approximately equal when the same total mass M of beads is placed in each of the two compartments (Fig. 8). However, for the same mass M, the pressure P is slightly larger for the much more numerous smaller beads; the conclusion is again in agreement with an increase in the slope T_P with ρ (Sec. III C 2). The result holds true for all the diameter differences explored experimentally (D ranging from 1.5 to 3.5 mm). One can also notice that the transition between the two regimes in $P(\Gamma)$ occurs at larger acceleration for the larger beads. As a consequence, ΔP becomes significant only when the acceleration is decreased below Γ_c for the larger beads.

The increase in Γ_c when D is increased is in agreement with a transition due to the existence of attractors to periodic motion at low accelerations (Sec. III C 2). Indeed, for the same mass M of beads, the number of the larger beads is less than that of the smaller beads; as a consequence, at a given acceleration, the bead-bead collision frequency is smaller for the larger beads. Since the bead-bead collisions destroy the coherence between the motions of the plate and of the beads [29], the existence of attractors to periodic motion is expected to come into play at a larger acceleration for the larger beads.

4. Pressure P versus restitution coefficient ϵ

We studied the dependence of the slope $dP/d\Gamma$ on ϵ by changing the material of the plate (Table I). We limited our measurements to large accelerations $\Gamma>\Gamma_c$, and large number density ρ so as to insure that the system was homoge-

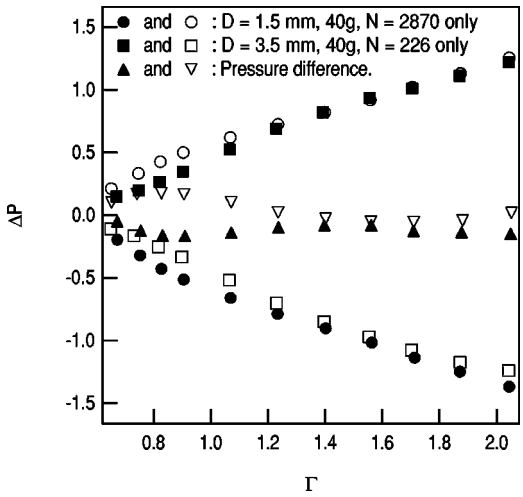

FIG. 8. Pressure difference ΔP vs acceleration Γ. Open symbols: the smaller beads in compartment A. Full symbols: the smaller beads in compartment B. The circles correspond to the pressure force applied by the smaller beads alone. The squares correspond to the pressure force applied by the larger beads alone. The triangles correspond to the pressure difference measured when the beads in compartments A and B strike the pendulum. The pressure force applied by the smaller beads is larger than that applied by the larger ones. The difference increases when the dimensionless acceleration is decreased (sine wave, 60 Hz, $M=40$ g, AISI, Dural tray).

neous. In these conditions, P is proportional to Γ, and the linear interpolation of the experimental results makes it possible to determine accurately the value of T_P extrapolated at $\Gamma=1$ (equivalent to the slope $dP/d\Gamma$) as a function of ϵ.

The experimental results are shown in Fig. 9; T_P^{-1} depends approximately linearly on ϵ so that $T_P \simeq T_P^0/[1+\zeta(1-\epsilon)]$ with $T_P^0=(2.7\pm0.2)\times10^{-3}$ m^{2}s^{-2} and $\zeta=5.5\pm0.5$. As expected, T_P decreases when ϵ is decreased. On the other hand, T_P seems to tend to the finite value T_P^0 in the limit $\epsilon\to1$. The asymptotic value T_P^0 and the parameter ζ are likely to depend on the bead-bead restitution coefficient e. The study of T_P^0

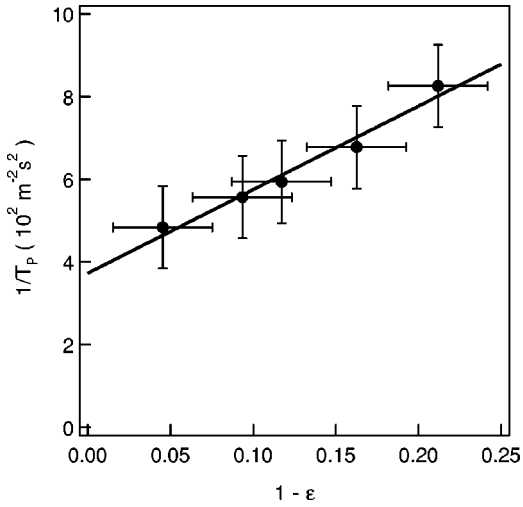

FIG. 9. T_P^{-1} vs $1-\epsilon$. Symbols: experimental data. Solid line: best linear fit. ($\rho=1.45\ 10^5\ m^{-2}$, steel beads, $D=2$ mm, sine wave 60 Hz).

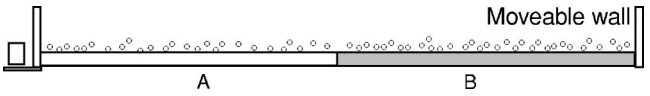

FIG. 10. Sketch of the experimental setup. The pendulum is removed. The vibrating plate is made of two different materials in two regions A and B that have the same surface area. For exactly the same characteristics of the vertical vibration, the difference $\Delta\epsilon$ between ϵ in A and B imposes, in the steady state, a difference between the number of beads N_A and N_B in the regions A and B. In order to conveniently measure the number N_B of beads in region B, one sidewall (on the right-hand side) can be easily removed.

and ζ as functions of e would be interesting as it would provide important information about the effect of the dissipation due to bead-bead collisions within the gas. However, this study would require accurate measurements of e as well as the ability to change e while keeping the same value of ϵ.

The dependence of T_P on ϵ will be further discussed by means of an additional experiment presented in the following section (III D).

D. Influence of the restitution coefficient ϵ: An additional study

We obtained more information about the influence of the restitution coefficients on the properties of the gas by measuring the density difference $\Delta\rho$ induced by a difference $\Delta\epsilon$ in ϵ between two different regions of the vibrating plate. In this study, the pendulum is removed, and we do not measure the granular pressure. However, the results, obtained in similar experimental conditions, reinforce the conclusions previously drawn out from the pressure measurements.

The experimental setup consists of a horizontal tray made of two different materials A and B having different restitution coefficients ϵ_A and ϵ_B (Fig. 10). Both regions have the same surface area $S=10\times10$ cm^2. Because of the significant difference in the density of the two materials A and B, the system must be adjusted carefully in order to insure that the vibration is truly vertical and that the vibration strength is constant over the whole surface of the tray. A given number N of glass beads is vibrated vertically until a steady state is reached. The system is quenched afterwards by suddenly setting the vibration amplitude to 0 (very few beads cross the border between the two different regions A and B during the cooling of the system). One of the four sidewalls can be easily removed in order to take and weight the beads on side B (Fig. 10). Thus the numbers N_A and N_B of beads in the regions A and B are easy to count. For a given difference $\Delta\epsilon$, the experiment is repeated for different values of Γ and N.

The typical experimental results are shown in Fig. 11. We report the percentage of beads in region A (B), $r_A \equiv 100N_A/N$ ($r_B \equiv 100N_B/N$) as a function of Γ for various N. Within the scatter of the experimental data, the results do not depend on N (or equivalently ρ). At large Γ, the difference r_B-r_A tends to a constant value, whereas it increases at small Γ; the number of beads then increases in the region that has the smallest ϵ. The departure from the constant density difference at low accelerations is not due to the appearance of a visible collapse [vertical lines in Fig. 11]. We observe that

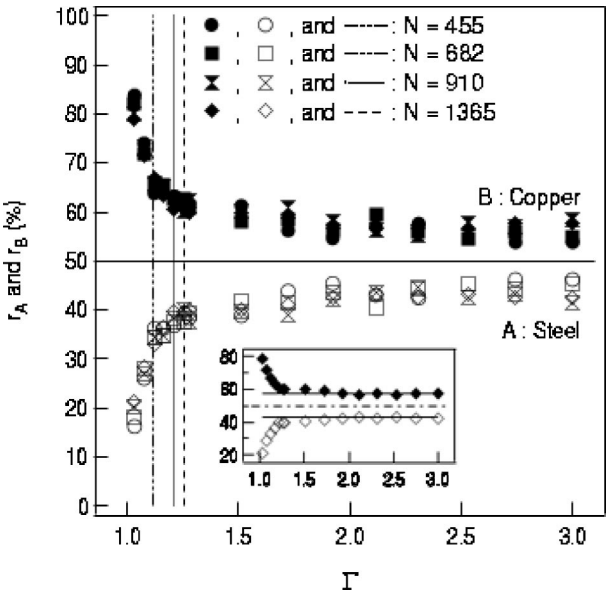

FIG. 11. Percentages r_A and r_B vs acceleration Γ. Open symbols: percentage r_A of beads on the steel plate. Full symbols: percentage r_B of beads on the copper plate. The vertical dashed lines mark the nucleation of a collapse on the copper plate. Inset: $N=1365$; the scatter of the experimental data is less when N is large; r_A and r_B tend to constant values at large acceleration Γ (sine wave, 60 Hz, glass beads, $D=2$ mm, $\epsilon_A \simeq 0.95$, $\epsilon_B \simeq 0.76$).

the nucleation of the collapse, which occurs at larger Γ when N is larger [in agreement with the results given in Sec. III B], does not have any effect on the curves $r_A(\Gamma)$ and $r_B(\Gamma)$.

We repeated the experiment, changing the material of the plate B and keeping the steel plate in A. In Fig. 12, we report the asymptotic difference $\Delta r=(r_B-r_A)$ at large Γ. The difference Δr increases with an increase in $\Delta\epsilon=\epsilon_A-\epsilon_B$. In spite of

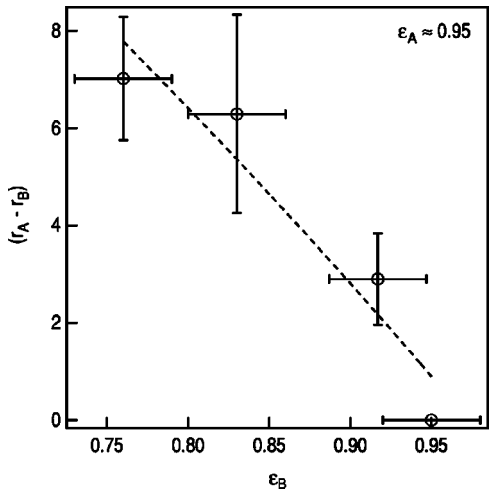

FIG. 12. Asymptotic difference $\Delta r=(r_B-r_A)$ vs ϵ_B. The difference Δr reported here accounts for the asymptotic density difference between regions A and B for four different total numbers of beads ($N=455$, 682, 910, or 1365). Assuming that $T_P \propto 1/[1+\zeta(1-\epsilon)]$ and that $P_A=P_B$, we obtain the best interpolation of the data (dashed line) with $\zeta \simeq 0.50 \pm 0.03$ (sine wave, 60 Hz, glass beads, $D=2$ mm).

the large error bars, the relation $T_P \propto 1/[1+\zeta(1-\epsilon)]$, with $\zeta \simeq 0.50 \pm 0.03$, and the assumption that the pressures are equal in regions A and B, account for the experimental results [dashed line in Fig. 12]. We note that the value of the parameter ζ is found to be much smaller for the glass-bead gas than that previously obtained with the system of steel beads ($\zeta \simeq 5.5$, Sec. III C 4). We do not have any explanation for this difference, and, missing reliable measurements of the bead-bead restitution coefficient e, we did not explore this point further.

However, the quantity Δr, which accounts for the density difference induced by a difference in ϵ between the regions A and B, does not significantly depend on ρ; this observation is in agreement with our previous conclusions, that P is approximately proportional ρ (Sec. III C 1, to within the slight increase in T_P with ρ, Sec. III C 2). At large accelerations, Δr tends to an asymptotic value, which increases with $\Delta\epsilon$, according to a decrease of T_G with ϵ (Sec. III C 4). At small accelerations, Δr increases significantly, the beads accumulating in the region having the smaller ϵ. The appearance of a visible collapse has no effect on the curve $\Delta r(\Gamma)$; this observation is again in agreement with the fact that the nucleation of a collapse has no effect on the curve $P(\Gamma)$ (Sec. III C 1).

IV. CONCLUSION

Our experimental findings can be summarized as follows:

(1) For a given vibration frequency ν, the granular pressure P increases with the acceleration Γ. We observe two different approximately linear regimes below and above a critical acceleration Γ_c which increases with both the frequency ν and bead diameter D. The transition is likely to be due to the presence of attractors to periodic motion at low accelerations.

(2) Up to coverage $C=0.5$, $T_P \equiv P/(m\rho)$ slightly increases with the number density ρ. Hence, the pressure P is not exactly proportional to ρ. At small coverages $C<0.5$, the improvement of the energy transfer from the vertical to the horizontal motion as the density is increased dominates the increase in the energy loss due to the bead-bead collisions.

(3) At a given dimensionless acceleration Γ, T_P decreases with the bead-plate restitution coefficient ϵ, according to $T_P \propto 1/[1+\zeta(1-\epsilon)]$.

(4) When the bead diameter D is changed, the granular pressure P at a given plate acceleration depends on the mass density M/S rather than on the number density ρ. We point out that thermalization by the vibrating boundary imposes T_P, and hence the mean square horizontal velocity of the beads, not their kinetic energy.

(5) The nucleation of the collapse occurs at larger accelerations when the density of the system is increased. However, once the collapse formed, the density of a granular gas does not significantly depend on the total number N of particles placed in the system.

Pressure measurements, performed with the help of a pendulum, provide reliable information on the steady state properties of 2D granular gases. Our experimental results suggest

that the transition at Γ_c is the clustering transition which is probably due to the existence of underlying attractors to periodic motion. It seems pertinent to simultaneously track both the vertical and horizontal motion of the particles and measure the pressure. These experiments could help discussing the relation between the distribution functions of, respectively, the vertical and horizontal velocities at small accelerations, and the transitions to the clustering phase and collapse.

[1] H. M. Jaeger, S. R. Nagel, and R. P. Behringer, Rev. Mod. Phys. **68**, 1259 (1996).
[2] L. P. Kadanoff, Rev. Mod. Phys. **71**, 435 (1999).
[3] H. J. Herrmann, S. Luding, and R. Cafiero, Physica A **295**, 93 (2001).
[4] J. Duran, *Sands, Powders, and Grains: An Introduction to the Physics of Granular Materials* (Springer, New York, 2000).
[5] B. N. J. Persson, *Sliding Friction, Physical Principles and Applications* (Springer, New York, 1998).
[6] C. S. Campbell, Annu. Rev. Fluid Mech. **22**, 57 (1990).
[7] Y. Du, H. Li, and L. P. Kadanoff, Phys. Rev. Lett. **74**, 1268 (1995).
[8] J. J. Brey, J. W. Dufty, C. S. Kim, and A. Santos, Phys. Rev. E **58**, 4638 (1998).
[9] T. P. C. van Noije and M. H. Ernst, Granular Matter **1**, 57 (1998).
[10] T. P. C. van Noije, M. H. Ernst, E. Trizac, and I. Pagonabarraga, Phys. Rev. E **59**, 4326 (1999).
[11] A. Puglisi, V. Loreto, U. Marini Bettolo Marconi, and A. Vulpiani, Phys. Rev. E **59**, 5582 (1999).
[12] M. P. Dudukovic, F. Larachi, and P. L. Mills, Chem. Eng. Sci. **54**, 1975 (1999); J. B. Joshi, *ibid.* **56**, 5893 (2001).
[13] I. S. Aranson, D. Blair, V. A. Kalatsky, G. W. Crabtree, W.-K. Kwok, V. M. Vinokur, and U. Welp, Phys. Rev. Lett. **84**, 3306 (2000).
[14] I. S. Aranson and J. S. Olafsen, e-print cond-mat/0110607v2.
[15] A. Kudrolli, M. Wolpert, and J. P. Gollub, Phys. Rev. Lett. **78**, 1383 (1997).
[16] A. Kudrolli and J. Henry, Phys. Rev. E **62**, R1489 (2000).
[17] J. S. Olafsen and J. S. Urbach, Phys. Rev. Lett. **81**, 4369 (1998).
[18] J. S. Olafsen and J. S. Urbach, Phys. Rev. E **60**, R2468 (1999).
[19] W. Losert, D. G. W. Cooper, A. Kudrolli, and J. P. Gollub, Chaos **9**, 682 (1999).
[20] W. Losert, D. G. W. Cooper, and J. P. Gollub, Phys. Rev. E **59**, 5855 (1999).
[21] X. Nie, E. Ben-Naim, and S. Y. Chen, Europhys. Lett. **51**, 679 (2000).
[22] E. Falcon, C. Laroche, S. Fauve, and C. Coste, Eur. Phys. J. B **3**, 45 (1998), and references therein.
[23] C. V. Raman, Phys. Rev. E **12**, 442 (1918); D. Tabor, Proc. R. Soc. London, Ser. A **192**, 247 (1948); W. Goldsmith, *Impact* (Arnold, London, 1960); K. L. Johnson, *Contact Mechanics* (Cambridge University Press, Cambridge, 1985); L. Labous, A. D. Rosato, and R. N. Dave, Phys. Rev. E **56**, 5717 (1997); G. Kuwabara and K. Kono, Jpn. J. Appl. Phys., Part 1 **26**, 1230, (1987).
[24] L. Kondic, Phys. Rev. E **60**, 751 (1999).
[25] B. Painter and R. P. Behringer, Phys. Rev. E **62**, 2380 (2000).
[26] A. Lorenz, C. Tuozzolo, and M. Y. Louge, Exp. Mech. **37**, 292 (1997).
[27] The appearance of parasitic mechanical resonances as well as the decrease of the pressure limit the study at high frequencies. On the other hand, the increase of the vibration amplitude, which cannot be larger than the distance between the bottom edge of the pendulum and the vibrating plate (the bead radius), avoids the study at low frequencies.
[28] J. M. Luck and A. Mehta, Phys. Rev. E **48**, 3988 (1993), and references therein.
[29] J.-C. Géminard and C. Laroche, Phys. Rev. E **68**, 031305 (2003).